

# SCISRS: Signal Cancellation using Intelligent Surfaces for Radio Astronomy Services

Zhibin Zou, Xue Wei, Dola Saha, Aveek Dutta

Department of Electrical & Computer Engineering  
University at Albany, SUNY, Albany, NY 12222 USA  
{zzou2, xwei4, dsaha, adutta}@albany.edu

Gregory Hellbourg

Department of Astronomy  
California Institute of Technology  
{ghellbourg}@astro.caltech.edu

**Abstract**—Recently, there has been great interest in facilitating coexistence of active and passive users of the electromagnetic (EM) spectrum, with the primary objective of higher spectral utilization. The major challenge for passive users, such as Radio Astronomy Services (RAS), is the need for extremely *quiet skies* to make astronomical observations with maximum sensitivity of the radio telescope. This is increasingly difficult to guarantee because of densification of allocated spectrum, exponential growth of ubiquitous wireless communication and out-of-band astronomical observations required to observe fast radio bursts. This requires either bidirectional collaboration between active and passive users or innovative signal processing at the telescope site to cancel any incident Radio Frequency Interference (RFI). In this work, we show the feasibility of such a paradigm, where RFI from airborne sources, *e.g.*, aircraft, LEO satellites, etc., is cancelled at the receiver of a Radio Telescope, by shaping the EM waveform by an array of Reconfigurable Intelligent Surfaces (RIS). In contrast to conventional beam-nulling applications for RIS, this method requires precise calculation of the phase and the amplitude of the reflected signal by the RIS in order to guarantee complete cancellation of the incident RFI. We simulate this approach in a practical setting to study its error performance and boundary conditions of the system parameters, that will lead to a demonstrable prototype in near future. Our results indicate that an RIS array with 364 elements can fully cancel RFI for ADS-B systems at an elevation of 60° and an altitude of 10000 m.

**Keywords**—Reconfigurable intelligent surfaces, Radio frequency interference cancellation, Radio astronomy services.

## I. INTRODUCTION

Radio Astronomy is a discovery-based science, which has revolutionized our understanding of the Universe through scientific observations across the electromagnetic (EM) spectrum. However, only 1-2% of the spectrum is allocated for science below 50 GHz where almost all of the commercial radio communication occurs. Therefore, it is increasingly essential to use spectrum other than the current allocation for astronomical observations for two main reasons: 1) red-shifting of spectral lines due to the expanding Universe and 2) broad bandwidth radio continuum observations can increase the signal-to-noise ratio of weak radio sources. Hence, radio telescopes are generally located in geographically isolated areas to avoid radio frequency interference (RFI) from human generated electromagnetic waves. However, no matter how remote, all radio astronomy sites across the world are vulnerable to growing RFI with increasing human population [1]. The threat to radio observations is even more with growing number

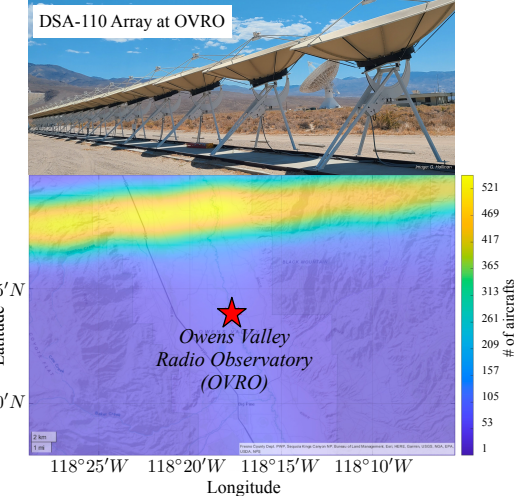


Fig. 1: Air traffic density around OVRO (red star). The aeronautical signals are observed as RFI at the Telescope.

of air- and space-borne transmitters as they directly radiate on the main beam of radio telescopes.

Figure 1 shows one such example of aeronautical activity in 1090 MHz from January to April 2022 around the Owens Valley Radio Observatory (OVRO) in California. It is one of the largest university-operated radio observatories in the world and hosts DSA-110 [2]. Deep Synoptic Array-110 (DSA-110) is a radio interferometer built for fast radio burst (FRB) detection and direct localization. It is under development to create an array of  $110 \times 4.65\text{m}$  dishes, which will continuously survey for FRBs. The next generation of radio telescope, DSA-2000 [3] will be even larger with 2000 dishes. Both DSA-110 and DSA-2000 suffer significantly from airborne RFI. To combat RFI, excision techniques involving lengthy post-processing are used, which significantly reduce the window of astronomical observations (40% data loss in L-band [4]). Although collaboration between active and passive usage has been suggested [5], it is not feasible for mobile transmitters where the process of collaboration through wireless media induces more RFI in Radio Astronomy Services (RAS). Hence, it is essential to innovate techniques that can intelligently detect RFI in real time and accurately cancel it at the radio telescope to preserve scientific observations in those electromagnetic bands.

Reconfigurable Intelligent Surface (RIS) [6], [7], has re-

cently become a topic of interest among researchers for improving the capacity of next generation wireless networks. RIS shapes the propagation environment into a desirable form by controlling the electromagnetic response of multiple scatters. Instead of scattered waves emanated from traditional antennas, the sub-wavelength separation between adjacent RIS elements enables the refracted and reflected waves to be generated via superposition of incident waves at the surface. Benefited from such a programmable characteristic to mold the wavefront into desired shapes, the RIS serves as a part of reconfigurable propagation environment where the received signals are directly reflected towards the receivers without cost of any extra power, thereby improving the link quality and coverage [8]. Encouraged by the promise of RIS in wireless communication systems, we investigated its feasibility to sculpt the wavefront to cancel RFI at the radio telescope.

We introduce SCISRS: Signal Cancellation using Intelligent SRadio Astronomy Services, which cancels incident RFI at the telescope receiver through creation of a destructive wavefront using a RIS. The proposed system is the first of its kind where RIS is used to cancel the energy of an RFI before it reaches the ADCs of the telescope, thus facilitating scientific broadband observations across the electromagnetic spectrum. Given a direction of arrival (DoA) of an RFI, SCISRS changes the phases of the RIS elements to steer the incident RFI towards telescope in order to cancel the incident interference at the telescope, thus dynamically creating a *EM quiet zone* around the receiver of the radio telescope. To realize this idea, we focus on the aeronautical signals from aircraft (960-1215 MHz) in L-band due to growing interest in observing the lower frequencies by the radio astronomy community. Figure 2 shows the system architecture with three entities: the telescope receiver, the RFI DoA Estimator and the RIS, which are together used to cancel the RFI transmitted by an airborne transmitter. The direct path of RFI (aeronautical signals) is incident on the telescope receiver, which undergoes flat fading channel, propagation loss and antenna sidelobe gain. Similarly, another direct path of the transmitter signal reaches the RIS unit. The reflected signal at the telescope is the collective sum of all signals reflected by multiple RIS cells, which has undergone a cascaded channel of Transmitter-RIS and RIS-Telescope. The RFI is cancelled at the radio telescope when both *the magnitude and phase response* of the RIS array exactly equals the channel and antenna gains of the direct path. Essentially, SCISRS makes passive radio telescope a cognitive system that can reflect incident RFI, dynamically creating an EM quiet zone to coexist with other important active wireless communications around it.

## II. RELATED WORK

**RFI mitigation in radio astronomy:** Active RFI mitigation has become a necessary practice in the radio astronomy community. Known persistent and fixed sources of RFI are highly attenuated at the front-end of the receiver using series of

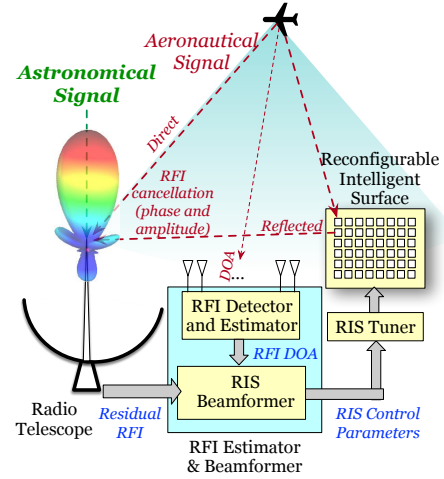


Fig. 2: SCISRS: Cancelling RFI from airborne transmitters at the radio telescope by reconfigurable intelligent surfaces.

analog superconductive filters [9], [10], but frequencies with high RFI density (e.g. FM or Digital Video Broadcast band) are usually simply avoided by design. Fast processors (RFSOC and FPGA) enable the detection and the blanking of impulsive RFI in the baseband digital samples, post-digitization [11], [12]. Data flagging consists of detecting time and frequency data corrupted with RFI, and discard them by replacing these values with zeros or random noise. This process occurs after channelization and time integration, where the intermediate telescope data product has the appropriate time resolution (of the order of 1 ms) to match most RFI duty cycles. This can be applied manually after a careful inspection of the collected data, but conventional data reduction software include automated flagger based on local and global statistics of a given dataset [13]. Research in RFI flagging has also resulted in the development of real-time “on-the-fly” data flaggers [14], and the use of machine learning to automatically recognize and classify detected RFI [15].

**RIS aided wireless communication and sensing:** RIS or Intelligent Reflecting Surface (IRS) has been considered as a key enabler for next generation wireless communication to improve coverage, capacity and secrecy by reducing energy consumption compared to active relays. Beamforming optimization [16] is formulated to minimize the transmit power at the access point by jointly optimizing the transmit precoding and the discrete reflect phase shifts at the IRS. RIS is combined with MIMO to increase system capacity [17] by optimizing transmit coefficients and covariance matrices. To reap the gains of RIS, channel estimation [18], [19] is essential, where the outdated estimates can be used effectively to improve system performance. Furthermore, RIS has been used to enhance physical layer security [20] by overlapping multiple signals at the eavesdropper. The RIS-aided system [21] has been shown to offer better performance in terms of physical layer security compared to traditional MIMO systems. RIS has also been used for human posture recognition [22] by actively customizing the electromagnetic

environment to achieve high recognition accuracy.

*Difference with prior work:* To the best of our knowledge, SCISRS is the first project that analyzes the feasibility to intelligently reflect electromagnetic waveforms to cancel RFI incident on the radio telescope. The major difference of our approach compared to prior work is that the transmitted signal cannot be modified or optimized based on the feedback from the receiver. At the telescope, the inaccuracy arises from location estimation of the transmitter, and the telescope receiver due to several factors, like vibrations, continuous motion, gravity on the feed, etc. The gains of the sidelobe of the telescope are difficult to estimate, leading to error in estimation of incident RFI. Hence, in this paper, we study the feasibility of using RIS to cancel RFI at the radio telescope.

### III. SIGNAL MODEL

Automatic Dependent Surveillance-Broadcast (ADS-B) is a cooperative surveillance technology for tracking aircraft. Through the on-board GPS and other systems, the position information (altitude, GPS coordinates, heading, etc.) can be obtained and broadcast through the communication equipment on the aircraft. Ground personnel can use proper equipment to receive this information and monitor or track the aircraft. ADS-B uses Pulse-Position Modulation (PPM) to transmit data. The most common ADS-B uses the mode-S extended squitter (downlink format 17) of the SSR transponder at 1090 MHz and 50 KHz of bandwidth [23]. SCISRS is designed to be waveform agnostic and does not require decoding of the ADS-B signal. It is entirely based on the concept of energy cancellation of two incident EM waves.

In ADS-B system, the received power of RFI, travelling from the transmitter (airplane) to the receiver (telescope) can be considered as a line-of-sight (LOS) path and can be represented using the Friis transmission formula,

$$P_R = P_T \frac{G_T G_R \lambda^2}{(4\pi d)^2} \quad (1)$$

where,  $P_T$  is the transmitter power,  $G_T$  is the gain of the transmitter and  $G_R = \int_{S_d} G(\theta) d\theta$  is the total gain of beam-forming pattern  $G(\theta)$  over direct path region  $S_d$  at receiver. After introducing RIS, the received signal  $y$  at the receiver can be represented as the sum of RFI (transmitted signal  $x$ ) from transmitter (LOS) and its delayed component from RIS with  $M$  elements, and can be represented as:

$$y = a_d e^{j\phi_d} x + \sum_{m=1}^M a_m e^{j\phi_m} x + v \quad (2)$$

where,  $a_d$  and  $\phi_d$  are the channel gain and phase shift of direct path.  $a_m$  and  $\phi_m$  are the channel gain and phase shift of reflected path from  $m^{\text{th}}$  RIS element, and  $v$  is the noise. Thus, perfect cancellation of RFI at telescope receiver can be achieved when the residual RFI, in both *phase* and *amplitude*, measured at the receiver is zero.

$$|a_d e^{j\phi_d} + \sum_{m=1}^M a_m e^{j\phi_m}| = 0 \quad (3)$$

Perfect RFI cancellation, as in equation (3), can be achieved by optimally controlling the delay and the active number of RIS elements according to geometric the relationship of transmitter, receiver and RIS.

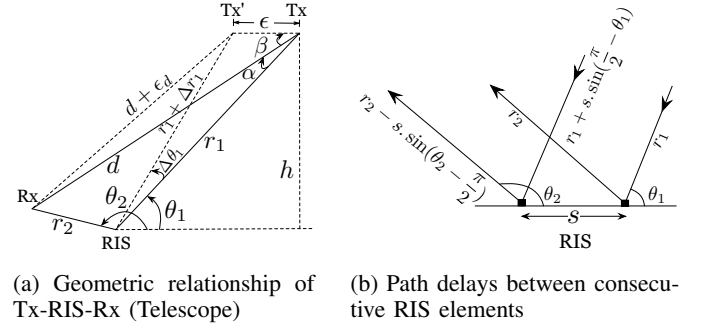


Fig. 3: Geometry of RIS and path delays

### IV. OPTIMAL RIS DESIGN FOR RFI CANCELLATION

The main objective of this work is to cancel RFI at the telescope receiver. In actual operation an *EM quiet zone* will be created around the telescope receiver, which signifies a *zero energy field* as a result of the cancellation of the two incident signals: a) the RFI and b) the RIS reflected waveform. Unlike National Radio Quiet zone, the *EM quiet zone*, is a targeted small area around the radio telescope receiver where there is no radio transmissions. In our work, we will dynamically create this quiet zone depending on the variations of the transmitter's signal and its position. In this section, we show the optimal phase and amplitude solutions for the RIS elements in order to achieve the envisioned EM quiet zone, represented by equation (3), and its boundary conditions.

#### A. Geometric estimation

Figure 3a shows the geometry of the three entities: the transmitter, the telescope receiver and the RIS. In this figure,  $r_2$  and  $\theta_2$  will vary as the telescope moves and scans the sky. However, they can be accurately estimated from the parameters shared by the telescope about its current position.  $\theta_1$  is the estimated DoA. Then, the distance of the direct path is  $d = \sqrt{r_1^2 + r_2^2 - r_1 r_2 \cos(\theta_2 - \theta_1)}$ . This is an essential component in estimating the phase and amplitude of the incident RFI at telescope. If the power and gain of the transmitter is denoted as  $P_T$  and  $G_T$  and the initial power of RFI incident at the receiver is  $P_R$  and at RIS with  $M$  elements is  $P_M$ , then we have,

$$\begin{aligned} \frac{P_R}{P_M} &= \frac{P_T \frac{G_T G_R \lambda^2}{(4\pi d)^2}}{P_T \frac{M^2 G_T G_r \lambda^2}{(4\pi r_1)^2}} = \frac{G_R r_1^2}{M^2 G_r d^2} \\ &= \frac{G_R r_1^2}{M^2 G_r \left[ r_1^2 + r_2^2 - r_1 r_2 \cos(\theta_2 - \theta_1) \right]} \end{aligned} \quad (4)$$

where,  $G_r$  is the gain of each RIS element. As  $r_1 \gg r_2 > 0$ , the quadratic solution for  $r_1$  in equation (4) is given by,

$$\begin{aligned} r_1 &= \frac{r_2 M}{2|P_R M^2 G_r - P_M G_R|} \\ &\quad \left\{ \sqrt{P_R^2 M^2 G_r^2 [\cos^2(\theta_2 - \theta_1) - 4] + 4 P_M G_R P_R G_r} \right. \\ &\quad \left. - \text{sgn}(P_R M^2 G_r - P_M G_R) P_R M G_r |\cos(\theta_2 - \theta_1)| \right\} \end{aligned} \quad (5)$$

## B. Phase solution

Since both the transmitter and the receiver are in the far-field of the RIS, we can consider that rays are incident in parallel, as shown in figure 3b. If  $s$  is the distance between the two consecutive elements of an RIS, then the total paths traversed due to reflection on the first and second elements are  $d_1 = r_1 + r_2$  and  $d_2 = r_1 + r_2 + s[\sin(\frac{\pi}{2} - \theta_1) - \sin(\theta_2 - \frac{\pi}{2})]$  respectively. Following the same derivation, the difference between the direct path ( $d$ ) and  $m^{\text{th}}$  element is,

$$\Delta d_m = r_1 + r_2 + s(m-1) \left[ \sin\left(\frac{\pi}{2} - \theta_1\right) - \sin\left(\theta_2 - \frac{\pi}{2}\right) \right] - d \quad (6)$$

The optimal phase solution in equation (3) is achieved when each reflected waveform has the opposite phase (phase difference is  $\pi$ ) to RFI. Therefore, we can write,

$$\text{mod}(\Delta\phi_m, 2\pi) = \pi \quad (7)$$

where,  $\Delta\phi_m$  is the phase difference between the  $m^{\text{th}}$  element and the RFI, caused by the path difference,  $\Delta d_m$  and the added delay,  $\tau_m$ ,

$$\Delta\phi_m = \phi_m - \phi_d = \frac{2\pi\Delta d_m}{\lambda} + \frac{2\pi c\tau_m}{\lambda} \quad (8)$$

Substituting equation (8) in equation (7), we have the closed form expression for  $\tau_m$  in equation (9)

$$\tau_m = \frac{(2K+1)\lambda - 2\Delta d_m}{2c} \quad (9)$$

where,  $K$  is the smallest integer that ensures  $\tau_m > 0$ .

## C. Amplitude Solution

As  $s \ll r_1 + r_2$ , the variation in reflected energy from different elements of RIS is negligible. If  $G'_R$  is the gain of the reflected beam, the power received by receiver from reflected path of each element is given by equation (10)

$$P'_R = P_T \frac{G_T G_r \lambda^2}{(4\pi r_1)^2} \cdot \frac{G_r G_{R'} \lambda^2}{(4\pi r_2)^2} = P_T \frac{G_T G_{R'} G_r^2 \lambda^4}{(16\pi^2 r_1 r_2)^2} \quad (10)$$

Meanwhile, applying the optimal delay derived in equation (9) to each RIS element, the reflected waveform from RIS has the opposite phase to RFI and thus equation (3) is rewritten as in equation (11)

$$a_d = \sum_{m=1}^M a_m = \sum_{n=1}^N a_n + \sum_{m=N+1}^M a_{m'} \quad (11)$$

where,  $a_d = \sqrt{P'_R}$  and  $a_n = \sqrt{P'_R}$ .  $N$  is the optimal number of active RIS elements.  $a'_{m'} = 0$  as We can turn off  $M-N$  elements by feeding the appropriate voltage to the PIN diodes in the RIS array. Then, the optimal number of elements is,

$$N = \frac{4\pi r_1 r_2}{\lambda d G_r} \rho \quad (12)$$

where,  $\rho = \sqrt{\frac{G_R}{G_{R'}}$  is the gain ratio. For a fixed  $G_r$ , in practice, we can only have the sub-optimal solution as in equation (13)}

$$N = \left\lfloor \frac{4\pi r_1 r_2}{\lambda d G_r} \rho + \frac{1}{2} \right\rfloor \quad (13)$$

Thus, to reduce the number of elements, the RIS can be located near the telescope receiver to reduce  $r_2$ . Furthermore,  $G_r$  will be guided by the metasurface used for reflection.

## V. ERROR BOUNDARY

Radio astronomy telescope receivers operate at extremely low SNR and any error in the cancellation process is detrimental to the system. SCISRS relies on estimates of various parameters to cancel RFI in phase and amplitude. Therefore, it is possible that a small error in any of these estimates can lead to residual RFI. The optimal design in § IV will have a crucial element of determining an error bound or error distribution based on certain physical phenomena that are beyond the control of the system.

### A. Phase Error

Given a location error of Tx,  $\{\Delta\theta_1, \Delta r_1\}$  (as in figure 3a), the induced phase error for the  $m^{\text{th}}$  RIS element is,

$$\epsilon_{\Delta\phi_m} = \frac{2\pi\epsilon_{\Delta d_m}}{\lambda} \quad (14)$$

where, error of reflected path difference,  $\epsilon_{\Delta d_m}$  is given by,

$$\begin{aligned} \epsilon_{\Delta d_m} &= r_1 + \Delta r_1 + r_2 \\ &\quad + s(m-1) \left[ \sin\left(\frac{\pi}{2} - \theta_1 - \Delta\theta_1\right) - \sin\left(\theta_2 - \frac{\pi}{2}\right) \right] \\ &\quad - (d + \epsilon_d) - \Delta d_m \\ &= \Delta r_1 + s(m-1) [\cos\theta_1 \cos\Delta\theta_1 \\ &\quad - \sin\theta_1 \sin\Delta\theta_1 - \cos\theta_1] - \epsilon_d \\ &\approx \Delta r_1 - s(m-1) \sin\theta_1 \Delta\theta_1 - \epsilon_d \end{aligned} \quad (15)$$

where, the direct path error  $\epsilon_d$  is given as

$$\epsilon_d = \sqrt{d^2 + \epsilon^2 - 2d\epsilon \cos\beta} - d, \quad \text{where,} \quad (16)$$

$$\epsilon = \sqrt{r_1^2 + (r_1 + \Delta r_1)^2 - 2r_1(r_1 + \Delta r_1) \cos\Delta\theta_1}$$

$$\beta = \arcsin\left(\frac{r_1 + \Delta r_1}{\epsilon} \sin\Delta\theta_1\right) - \arccos\left(\frac{r_1^2 + d^2 - r_2^2}{2r_1 d}\right)$$

For  $s \ll \Delta r_1 + \epsilon_d$ , phase error between elements can be neglected. Thus, the total phase error is approximated with the average phase error as

$$\epsilon_\phi \approx \frac{2\pi}{\lambda} \left( \Delta r_1 - \frac{Ns}{2} \sin\theta_1 \Delta\theta_1 - \epsilon_d \right) \quad (17)$$

The worst case is  $\text{mod}(\epsilon_\phi, 2\pi) = \pi$ , which means the reflected waveform will enhance RFI. We normalize the phase error as

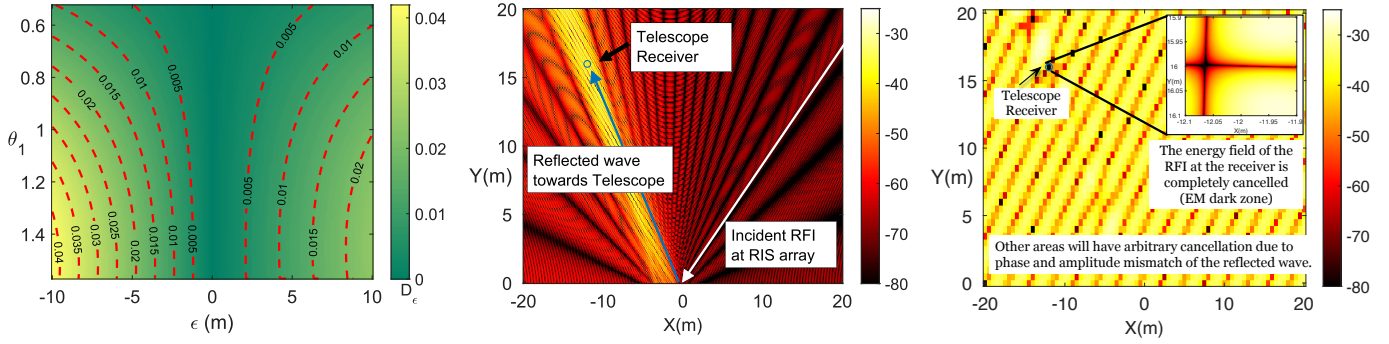
$$D_\epsilon = \frac{|\pi - |(\text{mod}(\epsilon_\phi, 2\pi) - \pi)||}{\pi} \quad (18)$$

where  $D_\epsilon = 0$  is the best case and  $D_\epsilon = 1$  is the worst case. These two cases indicate that the reflected waveform has exactly opposite phase and same phase as RFI, respectively.

### B. Power Error

The power error results from both the sub-optimal solution in equation (13) and location error  $\{\Delta\theta_1, \Delta r_1\}$ , given as

$$\begin{aligned} \epsilon_P &= \left| P_T G_T \lambda^2 \left\{ \left( \left\lfloor \frac{4\pi(r_1 + \Delta r_1)r_2}{\lambda d G_r(d + \epsilon_d)} \rho + \frac{1}{2} \right\rfloor \right)^2 \right. \right. \\ &\quad \left. \left. \cdot \frac{G_{R'} G_r^2 \lambda^2}{[16\pi^2(r_1 + \Delta r_1)r_2]^2} - \frac{G_R}{(4\pi d)^2} \right\} \right| \end{aligned} \quad (19)$$



(a) Phase error of the RIS reflected beam with respect to  $\epsilon$  and  $\theta_1$  (b) Energy field of the amplitude & phase adjusted RIS reflected beam (c) EM Quiet Zone: RFI is completely cancelled at the Telescope receiver

Fig. 4: Effect of error on EM Quiet Zone at the telescope

### C. Transition Error

Both path difference and the added delay can cause transition error  $\epsilon_L$ , where  $\epsilon_L$  caused by the added delay is negligible as we choose the smallest integer  $K$  in equation (9). With location error of transmitter, we have

$$\epsilon_L = r_1 + \Delta r_1 + r_2 - d \approx \Delta r_1 + r_2 < \epsilon + r_2 \quad (20)$$

It will cause catastrophic error if  $\epsilon_L > L$ , where  $L$  is the pulse length. For ADS-B, where pulse duration time is  $1 \mu\text{s}$ , we have  $L \approx 300 \text{ m}$ . As GPS can provide accuracy less than  $5 \text{ m}$  ( $\epsilon < 5 \text{ m}$ ) and RIS can be placed as close as  $5 \text{ m}$  ( $r_2 = 5 \text{ m}$ ) for DSA-110 and DSA-2000 dish with diameters  $\approx 5 \text{ m}$ , we have  $\epsilon_L < \epsilon + r_2 < L$ .

## VI. PERFORMANCE EVALUATION

### A. Simulation Setup

We simulate the whole transmission environment and evaluate RFI cancellation performance in MATLAB. The carrier frequency of ADS-B signals is  $f_c = 1090 \text{ MHz}$  and hence the wavelength is  $\lambda = c/f_c = 275 \text{ mm}$ . For the design of RIS elements, we choose  $\lambda/4$  as the size of each element of RIS, which is smaller than the wavelength. As for the spacing between two RIS elements, we choose  $\lambda/10$  so that if the spacing is large enough, the coupling effects are negligible. We set the height of flight,  $h$ , to be 10,000 meters and the distance between the telescope receiver and the RIS,  $r_2$ , to be 20 meters. This is specifically the distance between the rightmost element of the RIS and the telescope. We also set  $\theta_1$  and  $\theta_2$  to  $60^\circ$  and  $150^\circ$  respectively. It is worth mentioning that we consider the elevation angle to describe how high the transmitter is relative to the RIS. We set  $G_r = 4 \text{ dB}$ , which is the gain of each RIS element, and  $\rho = 1$ , meaning that we consider equal gain of direct and the reflected beam.

### B. Cancellation Performance

For ADS-B, we set the error in horizontal axis as  $\epsilon$ . In this paper, we measure  $\theta_1$  from  $\pi/6$  to  $\pi/2$ . It is to be noted here that two symmetric RISs can be build on both sides of the receiver. At any instance, only one of them can be used and the other one can be closed (whose  $\theta_1 > \pi/2$ ). The analysis of each side is the same. Figure 4a shows  $D_\epsilon$  with respect to

$\epsilon \in [-10, 10]$  and  $\theta_1 \in [\pi/6, \pi/2]$  when  $h = 10000 \text{ m}$ . We observe that  $D_\epsilon$  is not symmetric with respect to  $\epsilon$ . This is because symmetric errors,  $\pm\epsilon$ , do not result in the same  $\Delta r_1$  and  $\epsilon_d$ , as shown in figure 3a.

Figure 4b shows the energy field of the RIS reflected beam. We set RIS elements on the area near the origin point on the x-axis, and the telescope receiver position at (-12, 16), shown in a blue circle. The white line in the figure represents the incident RFI towards RIS arrays, and the blue line shows the wave reflected by the RIS towards the telescope, which can be obtained by controlling the RIS. This figure shows the energy distribution in the area around RIS and the telescope. According to the legend bar, the yellow area has higher energy than the red area, meaning that the energy reflected by RIS is concentrated at the angle at which the telescope receiver is. In other words, RIS elements are controlled to reflect the signal in a fixed direction, which is exactly towards the telescope. With proper phase shifting and correct number of RIS elements, the signals at the telescope receiver can be canceled by the signals reflected by RIS.

The result of the overlap of the energy from the flight transmitter and the energy reflected from the RIS is shown in the figure 4c. Based on our design, there should be a quiet zone at the position of the telescope receiver, because the signals from the transmitter should be canceled with the signals reflected from RIS with opposite phases but the same energy. Other areas will also have varying degrees of cancellation due to phase and amplitude mismatches. As the blue circle shown in the figure, the telescope position is exactly a dark spot, meaning that the energy field of the RFI at the receiver is completely canceled. We also zoom in on the quiet zone area, shown in the top right area of figure 4c. The telescope receiver is at (-12, 16). But, due to the error of the total number of RIS elements and numerical error, the quiet zone is achieved near (-12.06, 16).

### C. Required number of RIS elements

The reflected waveform from RIS should have the same power as RFI to achieve complete deconstruction, which is determined by active number of RIS elements. Though the power of RFI changed over the location of transmitter, we

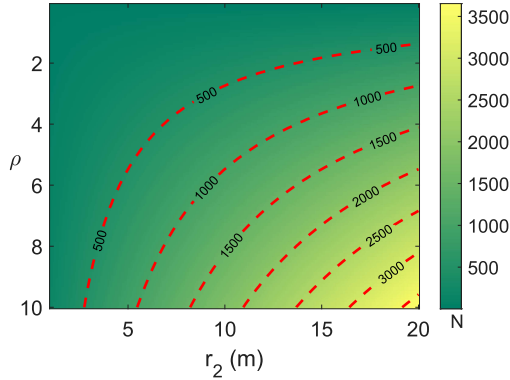


Fig. 5: Optimal number of active RIS elements.

can build RIS with maximal required number of RIS elements and dynamically turn off redundant elements according to DoA and transmit power in real-time. Figure 5 shows the optimal required number of RIS elements,  $N$ , as represented in equation (12) with respect to  $r_2$  and  $\rho$ . Given the diameter of DSA-110 and DSA-2000 dish antennas are  $\approx 5$  m, the RIS can be placed as close as 5 m away from the telescope receiver to reduce the required number of RIS elements.

## VII. IMPLEMENTATION INSIGHTS AND CONCLUSIONS

In this work, we showed that it is theoretically possible to find an amplitude and phase solution for each of the elements of an RIS array to precisely cancel the RFI at the telescope receiver with only the DoA and incident SNR of the signal, which is the first of its kind in the literature. However, we study the performance of the system under two major assumptions: 1) Error is considered only in elevation (or 2-D geometry for DoA and beamforming) and 2) DoA of the airborne transmitter is known. We are aware of the inaccuracies that may be induced as these assumptions are removed in practice. However, the underlying methodology for the amplitude and phase solutions will remain unchanged and is quite tractable for 3-D geometry as well. As ongoing work, the team is also developing novel two-stage DoA estimation algorithms that will yield better performance at low SNRs (far-away source) compared to known techniques like MUSIC, ESPRIT, etc.. Novel RIS fabrication methods are also being considered to allow for higher phase granularity (3-bit control) of the elements to precisely cancel the RFI. We believe that this work is a blueprint for practical system deployment and multidisciplinary research that will bridge the radio astronomy and the wireless communication research communities to collectively enhance spectrum utilization.

## VIII. ACKNOWLEDGEMENT

This work is funded by the National Science Foundation (Award # - 2128581 and 2229496).

## REFERENCES

- [1] I. A. Organisation, *Dark and Quiet Skies for Science and Society*, 2020. [Online]. Available: <https://www.iau.org/static/publications/dqsks-ies-book-29-12-20.pdf>
- [2] G. Hallinan and V. Ravi, "NSF Award # 1836018: The DSA: A Fast Radio Burst Localization Machine," [https://www.nsf.gov/awardsearch/showAward?AWD\\_ID=1836018](https://www.nsf.gov/awardsearch/showAward?AWD_ID=1836018).
- [3] G. Hallinan, V. Ravi, S. Weinreb, J. Kocz, Y. Huang, D. Woody, J. Lamb, L. D'Addario, M. Catha, J. Shi *et al.*, "The dsa-2000—a radio survey camera," *arXiv preprint arXiv:1907.07648*, 2019.
- [4] U. Rau, R. Selina, and A. Erickson, "Rfi mitigation for the ngvla: A cost-benefit analysis ngvla memo# 70," 2019.
- [5] M. Careem, S. Chakraborty, A. Dutta, D. Saha, and G. Hellbourg, "Spectrum sharing via collaborative rfi cancellation for radio astronomy," in *2021 IEEE International Symposium on Dynamic Spectrum Access Networks (DySPAN)*, 2021.
- [6] Q. Wu, S. Zhang, B. Zheng, C. You, and R. Zhang, "Intelligent reflecting surface-aided wireless communications: A tutorial," *IEEE Transactions on Communications*, vol. 69, no. 5, pp. 3313–3351, 2021.
- [7] Y. Liu, X. Liu, X. Mu, T. Hou, J. Xu, M. Di Renzo, and N. Al-Dhahir, "Reconfigurable intelligent surfaces: Principles and opportunities," *IEEE Communications Surveys Tutorials*, vol. 23, no. 3, pp. 1546–1577, 2021.
- [8] X. Cheng, Y. Lin, W. Shi, J. Li, C. Pan, F. Shu, Y. Wu, and J. Wang, "Joint optimization for rfs-assisted wireless communications: From physical and electromagnetic perspectives," *IEEE Transactions on Communications*, vol. 70, no. 1, pp. 606–620, 2022.
- [9] A. Soliman, S. Weinreb, G. Rajagopalan, C. Eckert, and L. Hilliard, "Quadrupole-ridged flared horn feed with internal rfi band rejection filter," in *2016 Radio Frequency Interference (RFI)*, 2016, pp. 115–116.
- [10] P. Bolli and F. Huang, "Superconducting filter for radio astronomy using interdigitated, capacitively loaded spirals," *Experimental Astronomy*, vol. 33, no. 1, pp. 225–236, 2012.
- [11] C. Dumez-Viou, R. Weber, and P. Ravier, "Multi-level pre-correlation rfi flagging for real-time implementation on uniboard," *Journal of Astronomical Instrumentation*, vol. 5, no. 04, p. 1641019, 2016.
- [12] D. Ait-Allal, C. Dumez-Viou, R. Weber, G. Desvignes, I. Cognard, and G. Theureau, "Rfi mitigation at nançay observatory: Impulsive signal processing," in *Widefield Science and Technology for the SKA SKADS Conference 2009*. ISBN 978-90-805434-5-4, 2010, pp. 201–205.
- [13] R. Urvashi, A. P. Rao, and N. Pune, "Automatic rfi identification and flagging," *The National Centre for Radio Astrophysics of the Tata Institute of Fundamental Research*, 2003.
- [14] A. Sclocco, D. Vohl, and R. V. van Nieuwpoort, "Real-time rfi mitigation for the apertif radio transient system," in *2019 RFI Workshop-Coexisting with Radio Frequency Interference (RFI)*. IEEE, 2019, pp. 1–8.
- [15] C. J. Wolfaardt, "Machine learning approach to radio frequency interference (rfi) classification in radio astronomy," Ph.D. dissertation, Stellenbosch: Stellenbosch University, 2016.
- [16] Q. Wu and R. Zhang, "Beamforming optimization for wireless network aided by intelligent reflecting surface with discrete phase shifts," *IEEE Transactions on Communications*, vol. 68, no. 3, pp. 1838–1851, 2020.
- [17] S. Zhang and R. Zhang, "Capacity characterization for intelligent reflecting surface aided mimo communication," *IEEE Journal on Selected Areas in Communications*, vol. 38, no. 8, pp. 1823–1838, 2020.
- [18] D. Shen and L. Dai, "Dimension reduced channel feedback for reconfigurable intelligent surface aided wireless communications," *IEEE Transactions on Communications*, vol. 69, no. 11, pp. 7748–7760, 2021.
- [19] Y. Zhang, J. Zhang, M. Di Renzo, H. Xiao, and B. Ai, "Reconfigurable intelligent surfaces with outdated channel state information: Centralized vs. distributed deployments," *IEEE Transactions on Communications*, vol. 70, no. 4, pp. 2742–2756, 2022.
- [20] Y. Ge and J. Fan, "Robust secure beamforming for intelligent reflecting surface assisted full-duplex miso systems," *IEEE Transactions on Information Forensics and Security*, vol. 17, pp. 253–264, 2022.
- [21] J. Zhang, H. Du, Q. Sun, B. Ai, and D. W. K. Ng, "Physical layer security enhancement with reconfigurable intelligent surface-aided networks," *IEEE Transactions on Information Forensics and Security*, vol. 16, pp. 3480–3495, 2021.
- [22] J. Hu, H. Zhang, B. Di, L. Li, K. Bian, L. Song, Y. Li, Z. Han, and H. V. Poor, "Reconfigurable intelligent surface based rf sensing: Design, optimization, and implementation," *IEEE Journal on Selected Areas in Communications*, vol. 38, no. 11, pp. 2700–2716, 2020.
- [23] R. S. Committee *et al.*, "Minimum aviation system performance standards for automatic dependent surveillance broadcast (ads-b)," Technical report, January, Tech. Rep., 1998.